energies

MDPI

Article

Multi-Objective Constructal Optimization for Marine Condensers

Huijun Feng [1,2,3], Wei Tang [4], Lingen Chen [1,2,3,*], Junchao Shi [4] and Zhixiang Wu [4]

1 Institute of Thermal Science and Power Engineering, Wuhan Institute of Technology, Wuhan 430205, China; huijunfeng@139.com
2 Hubei Provincial Engineering Technology Research Center of Green Chemical Equipment, Wuhan 430205, China
3 School of Mechanical & Electrical Engineering, Wuhan Institute of Technology, Wuhan 430205, China
4 College of Power Engineering, Naval University of Engineering, Wuhan 430033, China; 18202463039@163.com (W.T.); 18373248056@139.com (J.S.); zhixiangwuhg@outlook.com (Z.W.)
* Correspondence: lgchenna@yahoo.com or lingenchen@hotmail.com

Abstract: A marine condenser with exhausted steam as the working fluid is researched in this paper. Constructal designs of the condenser are numerically conducted based on single and multi-objective optimizations, respectively. In the single objective optimization, there is an optimal dimensionless tube diameter leading to the minimum total pumping power required by the condenser. After constructal optimization, the total pumping power is decreased by 42.3%. In addition, with the increase in mass flow rate of the steam and heat transfer area and the decrease in total heat transfer rate, the minimum total pumping power required by the condenser decreases. In the multi-objective optimization, the Pareto optimal set of the entropy generation rate and total pumping power is gained. The optimal results gained by three decision methods in the Pareto optimal set and single objective optimizations are compared by the deviation index. The optimal construct gained by the TOPSIS decision method corresponding to the smallest deviation index is recommended in the optimal design of the condenser. These research ideas can also be used to design other heat transfer devices.

Keywords: constructal theory; marine condenser; pumping power; entropy generation rate; multi-objective optimization; generalized thermodynamic optimization

Citation: Feng, H.; Tang, W.; Chen, L.; Shi, J.; Wu, Z. Multi-Objective Constructal Optimization for Marine Condensers. *Energies* **2021**, *14*, 5545. https://doi.org/10.3390/en14175545

Academic Editor: Victor Terekhov

Received: 26 July 2021
Accepted: 3 September 2021
Published: 5 September 2021

1. Introduction

A shell-and-tube heat exchanger (STHE) has the advantages of low cost, easy cleaning, large processing capacity, and reliable operation [1,2]. STHE is commonly used in marine condensers. Some researchers have conducted in-depth research on the STHE. Johnson et al. [3] studied the marine condenser with the goal of minimum total pumping power (TPP), and reduced the TPP by 35% after optimizing the external diameter and length of heat transfer tube (HTT). Patankar and Spalding [4], as well as Prithiviraj and Andrews [5], established the STHE models with a porous medium, and introduced the distributed resistance method to analyze the flow performances at shell side. Guo et al. [6] studied an STHE with different parameters and gained its optimal entropy generation performances under two different conditions. Mirzabeygi and Zhang [7] conducted multi-objective optimization of a surface condenser and obtained its optimal tube diameter, tube thickness, and tube spacing, respectively. Rodrigues et al. [8] proposed a new ecological function objective for evaluating the performance of an STHE and obtained the Pareto optimal solution set considering the new ecological function and total cost objective. Xiao et al. [9] minimized the total annual cost of an STHE network with phase change and reduced the cost of the network by up to 23.7%. Yu et al. [10] proposed a compound STHE with longitudinal vortex generator and pointed out that the rise in height and the attack angle of the generator could improve its overall performance. Sridhar et al. [11]

investigated the performance of an STHE with SnO_2-water and Ag-water nanofluids based on experimentation and found that thermal conductivity increased by 29% and 39% after adding the two nanoparticles, respectively. Li et al. [12] discussed the STHE arrangement problem for an organic Rankine cycle, and pointed out that the largest difference of the thermo-economic performance was 14.7% for the five considered STHE arrangements. Miansari et al. [13] studied the performance of an STHE with circular fins and pointed out that the circular fin had an obvious effect on the thermal efficiency of the STHE.

Constructal theory was proposed by Bejan [14], inspired from the formation of urban street network. The essence of constructal theory [15–28] can be described as: "For a finite-size flow system to persist in time (to live), its configuration must change in time such that it provides easier and easier access to its currents". The first engineering application of constructal theory was the heat dissipation of electronic devices [15], and the subsequent application of this theory opened up a new way for the designs and optimizations of various engineering processes and devices, including volume-point problems [29–33], cavities [34,35], heat sinks [25,36–39], heat sources [40,41], heat storage systems [42,43], energy conversion systems [44,45], civil constructions [46,47], steel structures [48,49], mechanical products [50,51], etc.

The heat exchanger (HE) is also the research object of constructal theory. On the basis of this theory, a group of scholars have carried out performance optimization research on HEs. Varga and Bejan [52] studied the performance of the HEs with fins and smooth surfaces and obtained the same optimal results for the two structures. Bejan [53] optimized the structure of a dendritic HE and gained the maximum heat transfer rate (HTR) density corresponding to the optimal construct of the HE. Da Silva et al. [54,55] and Zimparov et al. [56] further conducted constructal designs of various two-dimensional tree-shaped HEs and compared their performance under different flow patterns and shapes of HEs. Azad and Amipour [57] optimized the structure parameters of the HE with the goal of minimum total cost. They reduced the total cost of the HE by 50% after constructal optimization. Yang et al. [58,59] built a Y-shaped STHE model and evidently reduced the cost of the STHE after constructal optimization compared to that of the initial design. Mirzaei et al. [60] further conducted multi-objective optimization of the Y-shaped STHE model, and increased its thermal efficiency by more than 28%. Manjunath and Kaushik [61] further explored the heat transfer performance of an H-shaped HE and found that the comprehensive performance of the H-shaped HE was superior to that of the traditional HE. Bejan et al. [62] further optimized the construct of a cross-flow HE, obtained the optimal construct with the maximum HTR, and analyzed the influences of the total volume of the HE and the total number of flow channels on the constructal optimization results. Hajabdollahi [63] optimized a plate fin HE with multi-objective and obtained the optimal parameters about the fin and size of the HE. Ariyo and Bello-Ochende [64] optimized a subcooled microchannel HE and obtained the optimal performance of the microchannel better than that with single phase fluid. In addition, by applying constructal theory, the constructs of the regenerators [65,66], underground HEs [67,68], low temperature evaporators [69,70], steam evaporator [71], superheater [72] and economizer [73] of the boiler, biomass boilers [74,75], and steam generators, [76–79] were optimized, respectively.

Condenser is one of the usual HE types. It has also been optimized by few researchers using constructal design. Bejan et al. [80] optimized the arrangement of the tube bundles with the goal of maximum condensation rate of a condenser and obtained the optimal tube bundle arrangement and optimal condensation performance. Li et al. [81] performed constructal design of grooved condenser wick structures and formulated it as a general "area-to-point" heat conduction problem with disk-shaped structure.

The condenser is an important component of the marine steam power plant. The structure of the marine condenser has an important effect on its performance, which has not been optimized based on constructal theory in open published literatures. Therefore, a marine condenser will be researched in this paper. According to constructal law, in the conditions of fixed total HTR and heat transfer area (HTA), constructal design of the condenser will firstly be conducted with the goal of minimum TPP. The optimal outer diameter (OD) of the HTT will be obtained. The effects of cooling water inlet temperature (CWIT), steam mass flow rate (MFR), total HTA and HTR on constructal optimization results will be analyzed. Then, the multi-objective optimization considering the performances of entropy generation rate (EGR) and TPP will be further conducted, and the Pareto optimal set of the two indexes will be gained. The first novelty of this paper is the adoption of constructal theory in the performance of the marine condenser, which is expected to significantly improve its performance. Another novelty of this paper is the adoption of three decision methods to evaluate the Pareto optimal set gained by NSGA-II, which will choose a reasonable optimal design scheme for the marine condenser to satisfy different design requirements.

2. Model of the Marine Condenser

The simple model of a marine shell-and-tube condenser is shown in Figure 1. The exhausted steam enters from inlet 1 and flows through the outside of the HTT. The steam releases heat to the cooling water (CW), and finally flows out from exit 4. The CW (seawater) enters the HTTs of the condenser from inlet 5, absorbs heat from the steam, and then flows out from outlet 6. Since the heat transfer rates of the steam cooling and supercooling stages are small in the actual condenser, only the isothermal condensation process of the steam is considered in the simplified model. Thus, the working fluid is approximately viewed as the saturated states at inlet 1 and outlet 4. The corresponding T-s diagram is shown in Figure 2. The MFR of the CW and CWIT are $\dot{m}_c$ and $T_{c,in}$, respectively. The MFR, condenser pressure, and condensation temperature (CT) of the steam are $\dot{m}_{wf}$, P_s and T_s, respectively. The inner diameter, outer diameter, and number of the HTTs are $d_{c,in}$, $d_{c,out}$ and n, respectively. The path numbers at both sides are $N_{e,c}$ and $N_{e,wf}$, respectively. In the model, the influences of non-condensing gases and other factors are not considered. The heat loss of the condenser to external environment is ignored, thus the heat released by the exhausted steam is totally absorbed by the CW.

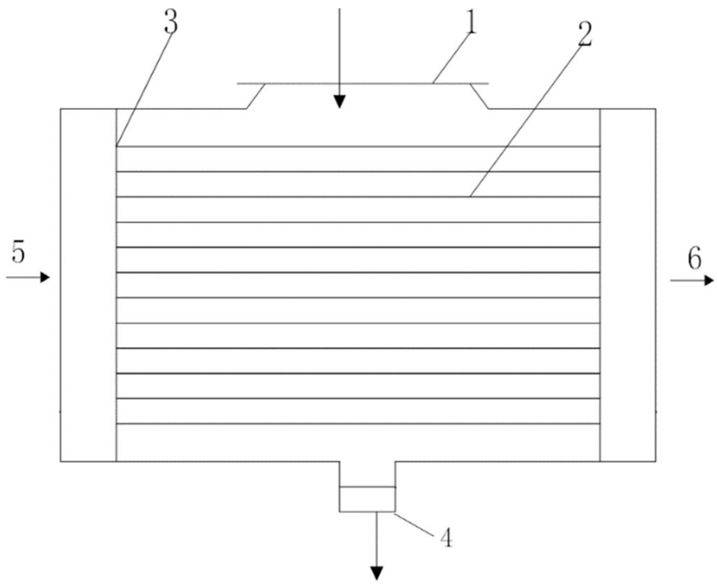

Figure 1. Simple model of a marine ST (1: exhausted steam inlet; 2: heat transfer tubes; 3: tube sheet; 4: condensed steam outlet; 5: cooling water inlet; 6: cooling water outlet).

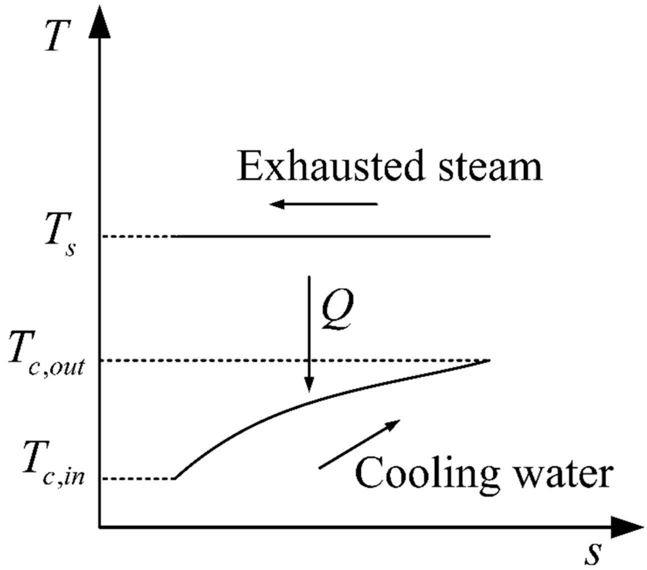

Figure 2. T-s diagram of heat exchange process in the condenser.

2.1. *Heat Transfer Calculation in Condenser*

2.1.1. Total HTR and Heat Balance Equation

The HTR (heat load) of the condenser is the heat transferred through the HTTs per unit time. The HTR of the condenser is calculated as

$$Q_c = KA_c\Delta T_m \tag{1}$$

where K is the total heat transfer coefficient (HTC), A_c is the total HTA, and ΔT_m is the logarithmic mean temperature difference (MTD).

The total HTA of the condenser is

$$A_c = \pi d_{c,out} l_c n_e \tag{2}$$

where n_e is the number of HTTs.

In the STHE, the temperature difference of the two fluids is not constant along the HTS. Therefore, the logarithmic MTD is introduced [82]

$$\Delta T_m = \frac{(T_s - T_{c,in}) - (T_s - T_{c,out})}{\ln \frac{(T_s - T_{c,in})}{(T_s - T_{c,out})}} \tag{3}$$

The HTR on the steam side is

$$Q_{c,wf} = \dot{m}_{wf} r_{LH} \tag{4}$$

where r_{LH} is the latent heat of the steam.

The HTR on the CW side is

$$Q_{c,water} = \dot{m}_c c_{pc} (T_{c,out} - T_{c,in}) \tag{5}$$

where c_{pc} is the specific heat capacity.

According to the energy conservation, the following equation should be satisfied

$$Q_c = Q_{c,wf} = Q_{c,water} \tag{6}$$

2.1.2. Total HTC

According to the heat transfer principle based on the multilayer wall, the total HTC is [83]

$$K_c = \frac{1}{\frac{d_{c,out}}{d_{c,in}\alpha_{c,water}} + \frac{d_{c,out}r_{e,in}}{d_{c,in}} + \frac{d_{c,out}\ln(d_{c,out}/d_{c,in})}{2\lambda_{c,wall}} + r_{e,out} + \frac{1}{\alpha_{c,wf}}} \tag{7}$$

where d_c is the diameter of the HTT, r_e is the fouling resistance of the HTT, $\lambda_{c,wall}$ is the thermal conductivity (TC) of the HTT, and α_c is the convective HTC, respectively.

Generally, the CW flowing in the tube is in a fully developed or turbulent state, therefore, the convective HTC on the inner surface of the HTT can be calculated by the Gnielinski formula [83]

$$\alpha_{c,water} = \frac{\lambda_{c,water}}{d_{c,in}} \cdot \frac{f_{c,water}/8\cdot(\mathrm{Re}_{c,water}-1000)\mathrm{Pr}_{c,water}}{1+12.7\sqrt{f_{c,water}/8}\left(\mathrm{Pr}_{c,water}{}^{2/3}-1\right)}\left[1+\left(\frac{d_{c,in}}{l_c N_{e,c}}\right)^{2/3}\right]\left(\frac{\mathrm{Pr}_{c,water}}{\mathrm{Pr}_{cw}}\right)^{0.01} \tag{8}$$

where $\mathrm{Re}_{c,water}$, $\mathrm{Pr}_{c,water}$, $\lambda_{c,water}$ and l_c are the Reynolds number, Prandtl number, TC, and length of the HTT, respectively. Furthermore, the resistance coefficient $f_{c,water}$ of the turbulent flow inside the tube is defined as

$$f_{c,water} = (1.82\lg\mathrm{Re}_{c,water} - 1.64)^{-2} \tag{9}$$

The condensation HTC at the exhausted steam side is formulated as [83]

$$\alpha_{c,wf} = 0.729\left[\frac{g r_{LH}\rho_l^2\lambda_l^3}{\nu_l d_{c,out}(T_s - T_w)}\right]^{\frac{1}{4}} \tag{10}$$

where g, r_{LH}, λ_l, ρ_l, ν_l, T_s and are the gravity acceleration, latent heat of vaporization, liquid film thermal conductivity, liquid film density, kinematic viscosity, steam temperature, and cooling wall temperature, respectively.

2.1.3. Total EGR

Ignoring the EGRs caused by the fluid flow and heat loss, the EGR at the exhausted steam side is

$$\Delta\dot{S}_{\mathrm{g,wf}} = \frac{\dot{m}_{wf}(h_{\mathrm{wf,in}} - h_{\mathrm{wf,out}})}{T_{\mathrm{s}}} \tag{11}$$

where $\dot{m}_{wf}$ is the MFR of the exhausted steam, T_{s} is the condensation temperature, and $h_{\mathrm{wf,in}}$ and $h_{\mathrm{wf,out}}$ are the inlet and outlet enthalpies of the exhausted steam, respectively.

The EGR for the heat absorbing process in HTTs is

$$\Delta\dot{S}_{\mathrm{g,c}} = \dot{m}_{\mathrm{c}}c_{pc}\ln(T_{\mathrm{c,out}}/T_{\mathrm{c,in}}) \tag{12}$$

Combining Equations (11) and (12), the total EGR of the condenser is

$$\dot{S}_{\mathrm{g}} = \Delta\dot{S}_{\mathrm{g,wf}} + \Delta\dot{S}_{\mathrm{g,c}} = \frac{\dot{m}_{wf}(h_{\mathrm{wf,in}} - h_{\mathrm{wf,out}})}{T_{\mathrm{s}}} + \dot{m}_{\mathrm{c}}c_{pc}\ln(T_{\mathrm{c,out}}/T_{\mathrm{c,in}}) \tag{13}$$

2.2. Calculations of Pressure Drop (PD) and Required TPP

For the HE, the TPP consumption is related with the PDs of the fluids in the tube and shell sides. Therefore, the PD is one of the important indicators to measure the HE performance.

The PD inside the tube is expressed as [82]

$$\Delta p_{c,water} = N_{e,c}\left(bl_c u_{c,water}{}^{1.75} + 0.135 u_{c,water}{}^{1.5}\right) \times 9.81 \tag{14}$$

where l_c is the length of tube, $u_{c,water}$ is the velocity, and b is the diameter correction factor.

The PD outside the tube is expressed as [82]

$$\Delta p_{c,wf} = 0.492 \times 10^{-3}\left(\frac{\dot{m}_{wf}\sqrt{v_{wf}}}{l_c d_{c,out}\sqrt{n_e}}\right)^{2.5} \tag{15}$$

where v_{wf} is the specific volume of the steam at the working fluid inlet of the condenser. Because the effect of the tube arrangement is not considered, the PD calculated in Equation (15) is an approximate value.

Combing Equations (11) and (12), the TPP required for the condenser is calculated as

$$W_c = \frac{\dot{m}_c \Delta p_{c,water}}{\eta_p \rho_{c,water}} + \frac{\dot{m}_{wf} \Delta p_{c,wf}}{\eta_p \rho_{c,wf}} \tag{16}$$

where η_p is the pump efficiency.

3. Constructal Design of the Marine Condenser

To study different performances of the marine condenser, constructal designs with single and multi-objective optimizations will be conducted in this section.

3.1. Constructal Design with Single Objective Optimization

The idea of the constructal design method is to find an optimal structure channel for a "flow" under the condition of a fixed structural constraint. Thus, the constructal design of the marine condenser in this paper is conducted by taking the TPP as the optimization objective and the tube diameter as the optimization variable with the constraints of constant heat load (HL) Q_c and total HTA A_c. The HTA constraint that reflects the investment cost of the condenser can be achieved by adjusting the length of the HTT when the tube diameter is varied. The TPP should be reduced as far as possible in the constructal design, which provides easier channels for the flows and reduces the operating cost of the condenser. To launch the constructal design of the marine condenser, the initial design parameters are given as: $N_{e,wf} = 1$, $N_{e,c} = 1$, $d_c = 0.016$ m, $T_{c,in} = 24$ °C and $Q_c = 53$ MW. These initial values are selected according to the actual engineering values and are not randomly selected. The dimensionless parameters used in the calculations are defined as: $\widetilde{A}_c = A_c/A_{c,\mathrm{int}}$, $\widetilde{d}_{c,out} = d_{c,out}/d_{c,\mathrm{int}}$, $\widetilde{m}_{wf} = \dot{m}_{wf}/\dot{m}_{wf,\mathrm{int}}$, $\widetilde{m}_c = \dot{m}_c/\dot{m}_{c,\mathrm{int}}$, $\widetilde{Q}_c = Q_c/Q_{c,\mathrm{int}}$ and $\widetilde{W}_c = W_c/W_{c,\mathrm{int}}$, where $A_{c,\mathrm{int}}$, $d_{c,\mathrm{int}}$, $\dot{m}_{wf,\mathrm{int}}$, $\dot{m}_{c,\mathrm{int}}$, $Q_{c,\mathrm{int}}$, and $W_{c,\mathrm{int}}$. These are the initial parameters and corresponding performances of the condenser, respectively.

Figure 3 shows the relationship between the dimensionless TPP $\widetilde{W}_c$ required by the condenser and the dimensionless tube diameter $\widetilde{d}_{c,out}$ when $T_{c,in} = 24$ °C. From Figure 3, as the dimensionless tube diameter $\widetilde{d}_{c,out}$ rises, the dimensionless TPP $\widetilde{W}_c$ sharply diminishes and then slowly rises. There is an optimum $\widetilde{d}_{c,out}$ ($\widetilde{d}_{c,out,opt} = 1.49$) leading to the minimum $\widetilde{W}_c$ ($\widetilde{W}_{c,m} = 0.577$). Compared with $\widetilde{d}_{c,out} = 1.0$, the TPP of the condenser is decreased by 42.3% after constructal optimization, which shows that the flow performance of the condenser can be greatly improved by selecting a suitable OD of the HTT. Moreover, the condensation temperatures (CTs) derived by the theoretical calculation (this paper) and real device (reference [82]) are 60.8 °C and 63.5 °C, respectively. This shows that the difference between them is small, which proves the correctness of the theoretical calculation results to some extent.

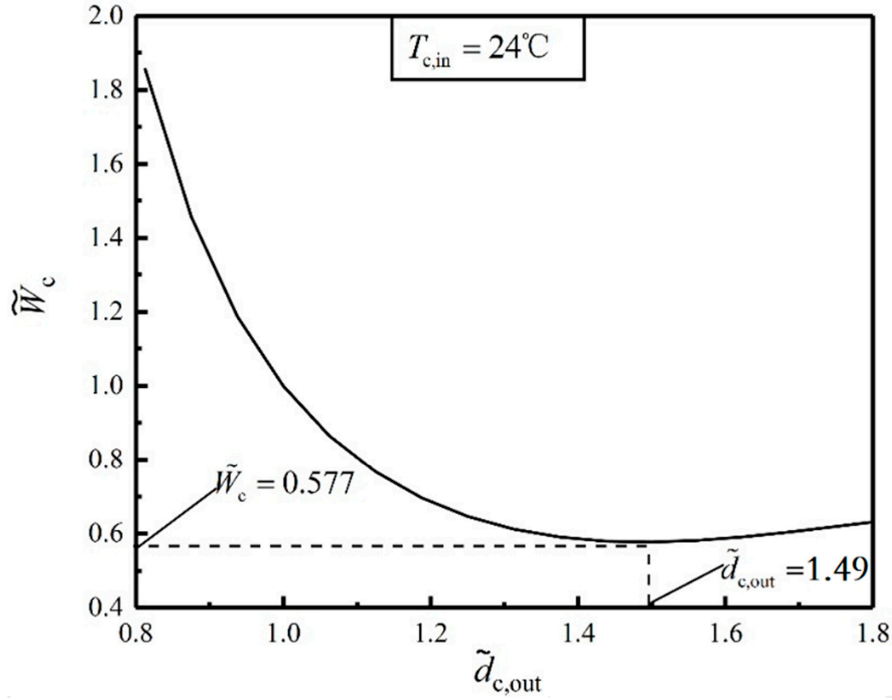

Figure 3. Relationship between $\widetilde{W}_c$ and $\tilde{d}_{c,out}$.

Figure 4 shows the influence of the CWIT $T_{c,in}$ on the relationship between the dimensionless TPP $\widetilde{W}_c$ of the condenser and dimensionless tube diameter $\tilde{d}_{c,out}$. From Figure 4, one can see that for the same tube diameter $\tilde{d}_{c,out}$, the dimensionless TPP $\widetilde{W}_c$ of the condenser with the CWIT $T_{c,in} = 22$ °C, is lower than those with the other discussed two temperatures. With the rise of CWIT $T_{c,in}$, the corresponding $\widetilde{W}_c$ rises gradually for the same $\tilde{d}_{c,out}$. The reason is that the rise of the CWIT $T_{c,in}$ reduces the MTD of the condenser. To achieve the design HL of the condenser, the CW flow rate must be increased, and the increase in the flow rate causes the increases of flow resistance and TPP. In addition, the CWIT has little effect on the optimum OD corresponding to the minimum TPP, thus the optimal structure of the condenser can be stably obtained according to its design standards.

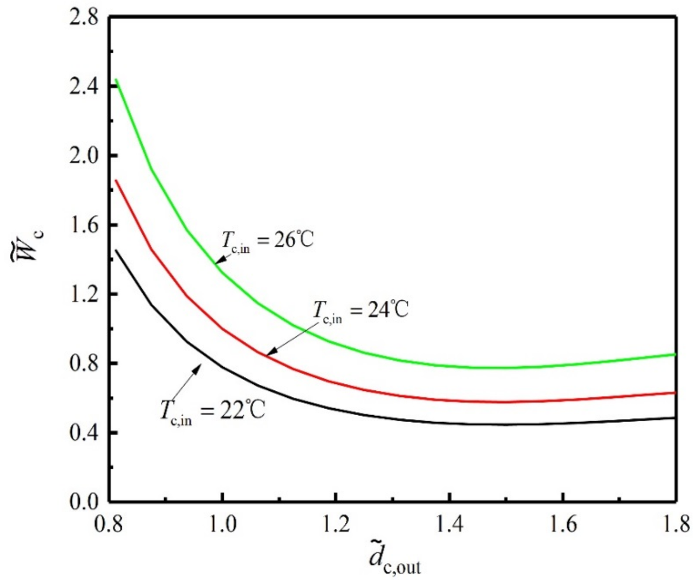

Figure 4. Influence of $T_{c,in}$ on the relationship between $\widetilde{W}_c$ and $\tilde{d}_{c,out}$.

Figure 5 shows the influences of the dimensionless MFR $\widetilde{m}_{wf}$ on the minimum dimensionless TPP $\widetilde{W}_{c,m}$ and optimal dimensionless tube diameter $\widetilde{d}_{c,out,opt}$. Figure 6 shows the influences of the dimensionless MFR $\widetilde{m}_{wf}$ on the dimensionless CT $\widetilde{T}_s$, outlet temperature $\widetilde{T}_{c,out}$ and MFR $\widetilde{m}_c$ of the CW at minimum TPP condition. Figure 5 illustrates that with the increase of $\widetilde{m}_{wf}$, $\widetilde{W}_{c,m}$ decreases gradually, $\widetilde{d}_{c,out,opt}$ increases as a whole, $\widetilde{T}_s$ and $\widetilde{T}_{c,out}$ increase, and $\widetilde{m}_c$ decreases. This is because under certain HL, the increase in steam MFR will inevitably lead to the decrease in condensation latent heat of the steam, and eventually the CT increases. When the MTD and HL are constants, the increase in CT will inevitably lead to the increases of average temperature and outlet temperature of the CW, and the MFR of the CW and the corresponding TPP ultimately reduce.

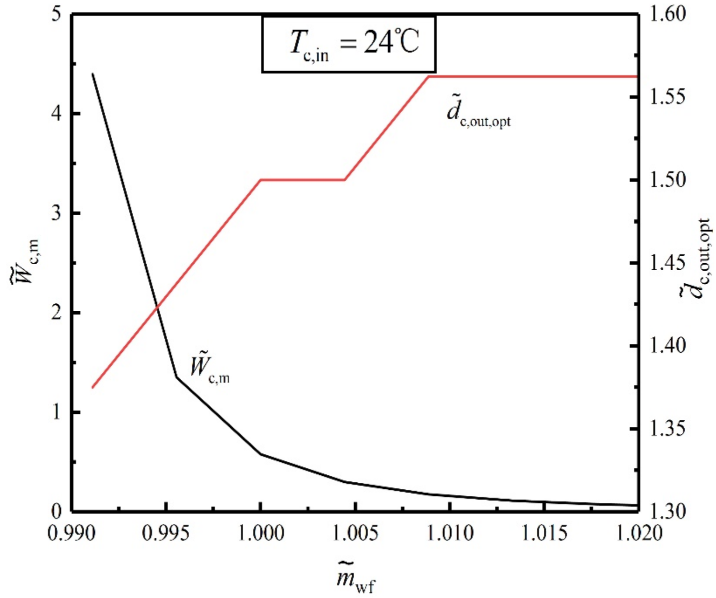

Figure 5. Influences of $\widetilde{m}_{wf}$ on the $\widetilde{W}_{c,m}$ and $\widetilde{d}_{c,out,opt}$.

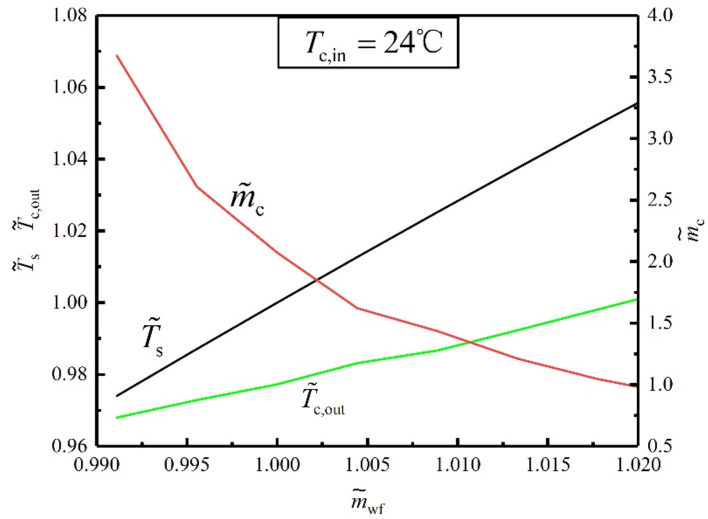

Figure 6. Influences of $\widetilde{m}_{wf}$ on the $\widetilde{T}_s$, $\widetilde{T}_{c,out}$ and $\widetilde{m}_c$.

Figures 7–10 show the influences of the dimensionless total HTA $\widetilde{A}_c$ and dimensionless HTR $\widetilde{Q}_c$ on the $\widetilde{W}_{c,m}$, $\widetilde{d}_{c,out,opt}$, $\widetilde{T}_s$, $\widetilde{T}_{c,out}$, and $\widetilde{m}_c$, respectively. One can find from the figures that the minimum dimensionless TPP $\widetilde{W}_{c,m}$ diminishes with the rise of $\widetilde{A}_c$, and the optimum dimensionless tube OD $\widetilde{d}_{c,out,opt}$ remains unchanged with the rise of $\widetilde{A}_c$, which indicates that increasing HTA is beneficial to reduce the TPP required by the condenser. The minimum dimensionless TPP increases sharply with the rise of dimensionless HTR $\widetilde{Q}_c$. In addition, with the rise of $\widetilde{Q}_c$, $\widetilde{d}_{c,out,opt}$ shows a downward trend. The dimensionless CT $\widetilde{T}_s$ under the minimum dimensionless TPP condition is less affected by $\widetilde{A}_c$, but decreases with the rise of $\widetilde{Q}_c$. $\widetilde{T}_{c,out}$ increases with the rise of $\widetilde{A}_c$, and gradually diminishes with the rise of $\widetilde{Q}_c$. $\widetilde{m}_c$ diminishes with the rise of $\widetilde{A}_c$, and increases with the rise of $\widetilde{Q}_c$. This is because under certain HL, increasing the total HTA means that the MTD between the steam and CW will diminish. When the CT changes little, the outlet temperature of the CW will increase, which ultimately leads to the decreases of the MFR and corresponding TPP. When the steam MFR is unchanged, increasing the HL means that the condensation latent heat of the steam needs to be increased and the CT is diminished correspondingly. Meanwhile, when the HTC and HTA are constants, the MTD will increase. This reduces both the average temperature and outlet temperature of the CW, and ultimately leads to the increases in the MFR and corresponding TPP.

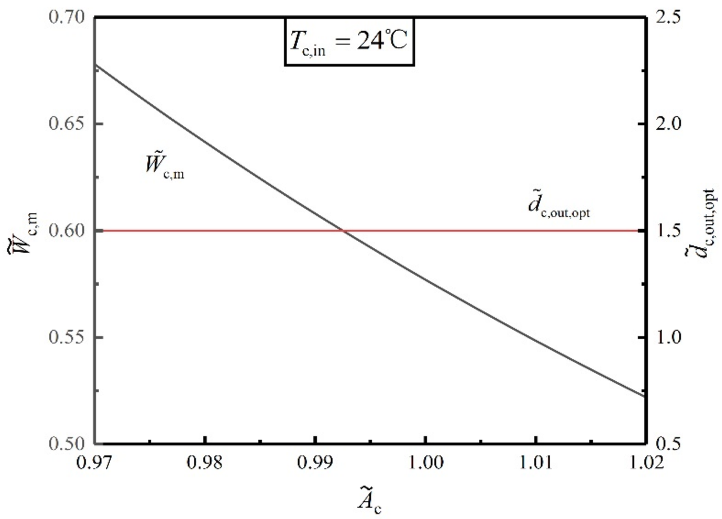

Figure 7. Influences of $\widetilde{A}_c$ on the $\widetilde{W}_{c,m}$ and $\widetilde{d}_{c,out,opt}$.

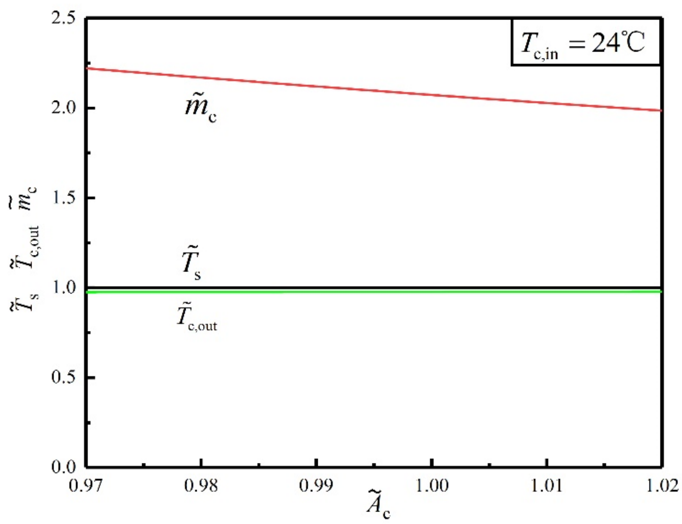

Figure 8. Influences of $\widetilde{A}_c$ on the $\widetilde{T}_s$, $\widetilde{T}_{c,out}$ and $\widetilde{m}_c$.

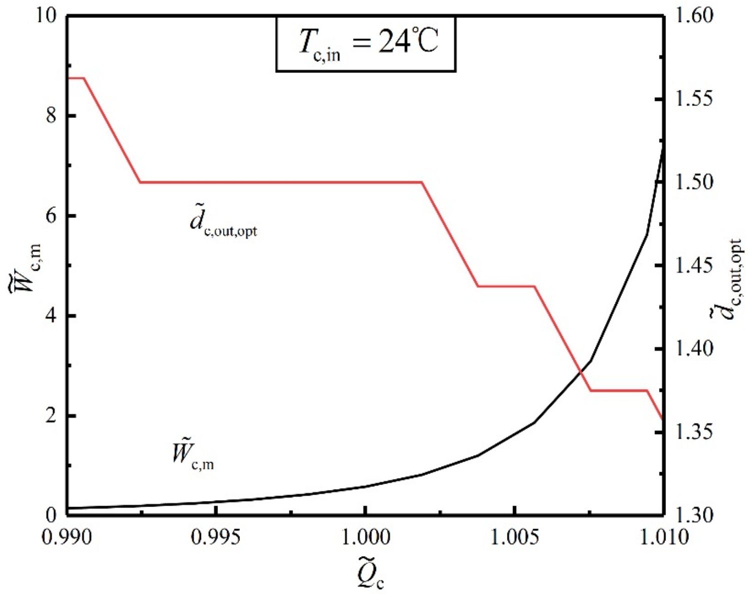

Figure 9. Influences of $\widetilde{Q}_c$ on the $\widetilde{W}_{c,m}$ and $\widetilde{d}_{c,out,opt}$.

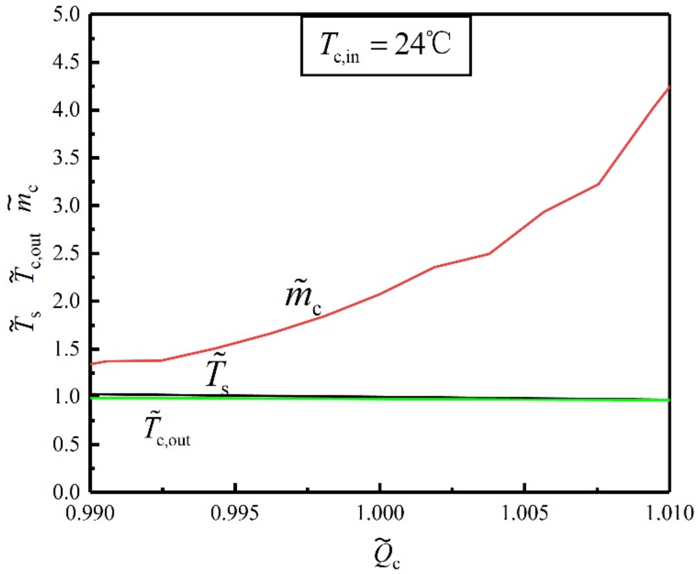

Figure 10. Influences of $\widetilde{Q}_c$ on the $\widetilde{T}_s$, $\widetilde{T}_{c,out}$ and $\widetilde{m}_c$.

3.2. Constructal Design with Multi-Objective Optimization

In the previous section, the TPP of the condenser is minimized. In effect, the EGR performance is another important index for the condenser. The performances of the EGR and TPP cannot reach the minimum at the same time, thus the multi-objective optimization is conducted in this section.

The flow chart of the multi-objective optimization is shown in Figure 11. From this figure, the dimensionless EGR ($\widetilde{S}_g = \dot{S}_g/\dot{S}_{g,int}$) and dimensionless TPP ($\widetilde{W}_c$) are taken as the two sub-objectives, and the dimensionless OD ($\widetilde{d}_{c,out}$) is taken as the optimization variable. The range of the optimization variable is set as: $0.8 \le \widetilde{d}_{c,out} \le 1.8$. The constraints of constant HL (Q_c) and total HTA (A_c) are considered, and the NSGA-II [84–106] is adopted in the optimization to search the Pareto front. The Pareto optimal set of $\widetilde{S}_g$ and $\widetilde{W}_c$ can be gained, and three decision methods can be used to evaluate the Pareto optimal set with the smallest deviation index. Figure 12 further shows the flow chart of the NSGA-II. In the NSGA-II, the population number, mutation probability, and generation number are set as 100, 0.9, and 20, respectively. When the maximum generation number is reached, the Pareto front can be exported.

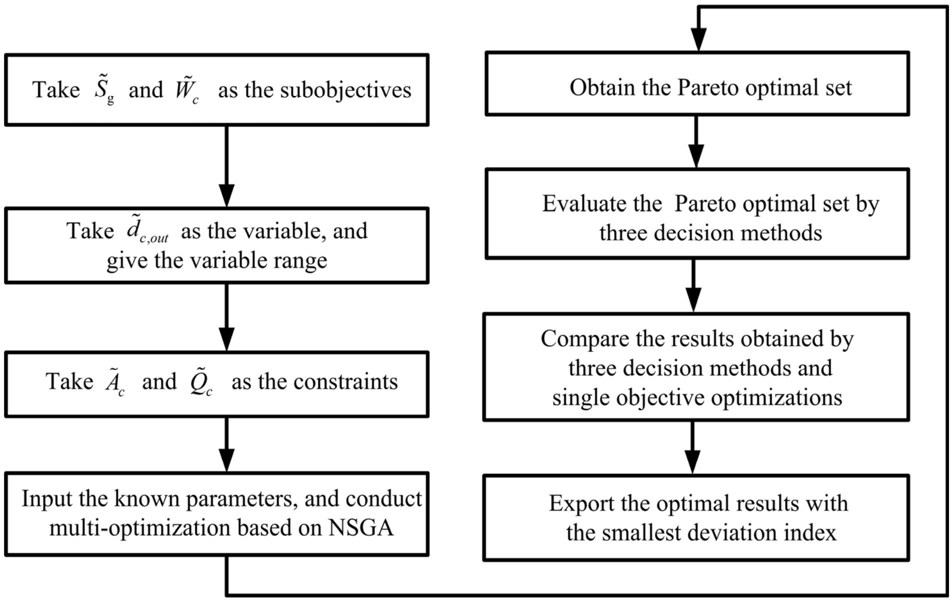

Figure 11. Flow chart of the multi-objective optimization.

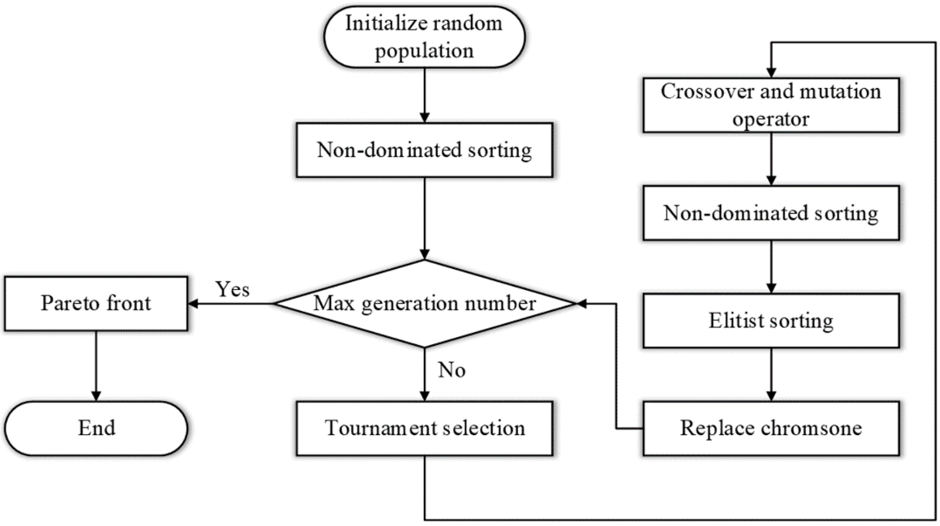

Figure 12. Flow chart of the NSGA-II.

Figure 13 shows the Pareto optimal set of $\widetilde{S}_g$ and $\widetilde{W}_c$ gained by multi-objective optimization. There are 100 points to describe the Pareto optimal set, which is represented by the blue symbol of "*" in Figure 13. From Figure 13, the Pareto optimal set locates between the ideal solution (point C) and nadir solution (point D), which is the compromise between the EGR and TPP under different design requirements. To compare the optimal results of the Pareto optimal set, the decision methods of LINMAP, TOPSIS, and Shannon entropy [84–104] are introduced. Table 1 lists the optimization results of the condenser gained by different decision methods and single objective optimizations. Obviously, the EGRs (or TPPs) of the condenser gained by the three decision methods are not smaller than those gained by EGR (or TPP) minimization at point A (or point B). One can further adopt the deviation index D_i to evaluate the optimization results. It shows that the deviation index of the TOPSIS decision method is the smallest one in Table 1. Therefore, the optimal construct gained by the TOPSIS decision method is recommended in the optimal design of the condenser.

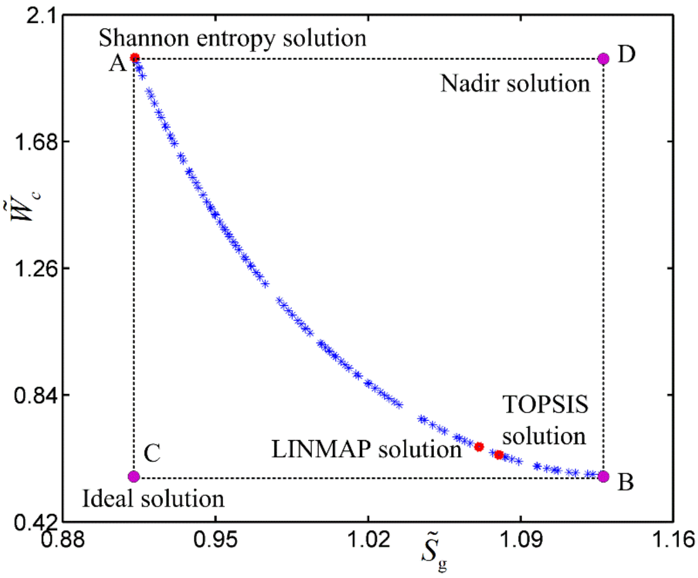

Figure 13. Pareto optimal front of $\widetilde{S}_g$ and $\widetilde{W}_c$ gained by multi-objective optimization.

Table 1. Optimization results gained by single and multi-objective optimizations.

Optimization Methods		Optimization Results $\widetilde{d}_{c,out}$	$\widetilde{S}_g$	$\widetilde{W}_c$	Deviation Index $\widetilde{D}_i$
Multi-objective Optimizations	LINMAP	1.22	1.071	0.668	0.124
	TOPSIS	1.26	1.080	0.642	0.120
	Shannon Entropy	0.80	0.913	1.958	0.865
Single Objective Optimizations	$\widetilde{S}_{g,min}$	0.80	0.913	1.958	0.865
	$\widetilde{W}_{c,min}$	1.49	1.128	0.577	0.134

4. Conclusions

Constructal design of a marine condenser is conducted in this paper. The TPP required by the condenser is minimized with fixed total HTR and HTA, and the optimal OD of the HTT is obtained. The multi-objective optimization considering the performances of EGR and TPP is further conducted, and the Pareto optimal set of the two indexes is gained. The results reveal that:

(1) There is an optimal dimensionless tube diameter $\widetilde{d}_{c,out,opt} = 1.49$ leading to the minimum TPP required by the condenser. Compared with $\widetilde{d}_{c,out} = 1.0$, the TPP of the condenser is reduced by 42.3% after constructal optimization, which greatly improves the fluid flow performance and reduces the operation cost of the condenser. As the steam MFR and HTA increase and the total HTR decreases, the minimum TPP required by the condenser decreases.

(2) The Pareto optimal set of the $\widetilde{S}_g$ and $\widetilde{W}_c$ gained by multi-objective optimization is the compromise between the EGR and TPP under different design requirements. The EGRs (or TPPs) of the condenser gained by the three decision methods are not smaller than that gained by EGR (or TPP) minimization at point A (or point B). The deviation index of the TOPSIS decision method is the smallest one. Therefore, the optimal construct gained by the TOPSIS decision method is recommended in the optimal design of the condenser.

The constructal design method, which is adopted in this paper, can be used as a theoretical instruction for optimal designs of various condensers. The next step is to consider more structure variables, such as the number, spacing, and arrangement of the

HTTs, to further improve the performance of the condenser. Furthermore, a more practical non-isothermal condensation model will be established with CFD software. All of these works can make the optimization research of the condenser more meaningful. The research model and optimized results can also be used to guide the modelling and optimization of the whole steam power plant.

Author Contributions: Conceptualization, H.F., W.T., and L.C.; Data curation, J.S., and Z.W.; Funding acquisition, L.C.; Methodology, H.F., W.T., L.C., and H.F.; Software, W.T., J.S., H.F., and Z.W.; Supervision, L.C.; Validation, H.F., W.T., and Z.W.; Writing—original draft preparation, H.F., and W.T.; Writing—reviewing and editing, L.C. All authors have read and agreed to the published version of the manuscript.

Funding: This work is supported by the National Natural Science Foundation of China (Grant Nos. 51779262, 52171317, and 51979278).

Institutional Review Board Statement: Not applicable.

Informed Consent Statement: Not applicable.

Data Availability Statement: Not applicable.

Acknowledgments: The authors wish to thank the reviewers for their careful, unbiased, and constructive suggestions, which led to this revised manuscript.

Conflicts of Interest: The authors declare no conflict of interest.

Nomenclature

A	Heat transfer area (m^2)
b	Diameter correction factor
c	Specific heat capacity (KJ/(kg·K))
d	Diameter (m)
g	Gravity acceleration (m/s^2)
K	Heat transfer coefficient ($W/(m^2 \cdot k)$)
l	Tube length (m)
$\dot{m}$	Mass flow rate (kg/s)
N	Path number
n	Tube number
Pr	Prandtl number
p	Pressure (Pa)
Q	Heat transfer rate (W)
Re	Reynolds number
r_{LH}	Latent heat (KJ/kg)
$\dot{S}_g$	Entropy generation rate (W)
T	Temperature (K)
u	Velocity (m/s)
v	Specific volume (m^3/kg)
W_c	Pumping power (W)
Greek letters	
α_c	Convective heat transfer coefficient ($W/(m^2 \cdot K)$)
η_p	Pump efficiency
$\lambda_{c,wall}$	Thermal conductivity of the tube (W/(m·K))
λ_l	Liquid film thermal conductivity (W/(m·K))
ν_l	Kinematic viscosity (m^2/s)
ρ_l	Liquid film density (kg/m^3)

Subscripts

c	Cooling water
in	Inlet
int	Initial
LH	Latent heat
m	Minimum
opt	Optimal
out	Outlet
p	Pump
s	Steam
wf	Working fluid
Superscripts	
$\sim$	Non-dimensionalized

Abbreviations

CT	Condensation temperature
CW	Cooling water
CWIT	Cooling water inlet temperature
EGR	Entropy generation rate
HE	Heat exchanger
HL	Heat load
HTA	Heat transfer area
HTC	Heat transfer coefficient
HTR	Heat transfer rate
HTT	Heat transfer tube
MFR	Mass flow rate
MTD	Mean temperature difference
OD	Outer diameter
PD	Pressure drop
STHE	Shell-and-tube heat exchanger
TC	Thermal conductivity
TPP	Total pumping power

References

1. Silaipillayarputhur, K.; Khurshid, H. The design of shell and tube heat exchangers—A review. *Int. J. Mech. Prod. Eng. Res. Dev.* **2019**, *9*, 87–102.
2. Kumar, S.; Singh, D. A Review on design and optimization of shell and tube heat exchanger by varying parameters. *Smart Moves J. Ijosci.* **2021**, *6*. Available online: https://ijoscience.com/ojsscience/index.php/ojsscience/article/view/298 (accessed on 1 September 2021). [CrossRef]
3. Johnson, C.M.; Vanderplaats, G.N.; Marto, P.J. Marine condenser design using numerical optimization. *J. Mech. Design* **1980**, *102*, 469–475. [CrossRef]
4. Patankar, S.V.; Spalding, D.B. A calculation procedure for transient and stead state behavior of shell-and-tube heat exchanger. *Heat Exch. Des. Theor. Source Book* **1974**, *1*, 155–176.
5. Prithiviraj, M.; Andrews, M.J. Three dimensional numerical simulation of shell-and-tube heat exchangers. Part I: Foundation and fluid mechanics. *Numer. Heat Transf. Part A Appl.* **1998**, *33*, 799–816. [CrossRef]
6. Guo, J.F.; Cheng, L.; Xu, M.T. Optimization design of shell-and-tube heat exchanger by entropy generation minimization and genetic algorithm. *Appl. Therm. Eng.* **2009**, *29*, 2954–2960. [CrossRef]
7. Mirzabeygi, P.; Zhang, C. Multi-objective optimization of a steam surface condenser using the territorial particle swarm technique. *J. Energy Res. Technol.* **2016**, *138*, 052001. [CrossRef]
8. Rodríguez, M.B.R.; Rodríguez, J.L.M.; Fontes, C.H.D.O. Thermo ecological optimization of shell-and-tube heat exchangers using NSGA II. *Appl. Therm. Eng.* **2019**, *156*, 91–98. [CrossRef]
9. Xiao, W.; Wang, K.; Jiang, X.; Li, X.; Wu, X.; Hao, Z.; He, G. Simultaneous optimization strategies for heat exchanger network synthesis and detailed shell-and-tube heat-exchanger design involving phase changes using GA/SA. *Energy* **2019**, *183*, 1166–1177. [CrossRef]
10. Yu, C.; Zhang, H.; Zeng, M.; Wang, R.; Gao, B. Numerical study on turbulent heat transfer performance of a new compound parallel flow shell and tube heat exchanger with longitudinal vortex generator. *Appl. Therm. Eng.* **2020**, *164*, 114449. [CrossRef]
11. Sridhar, S.V.; Karuppasamy, R.; Sivakumar, G.D. Experimental investigation of heat transfer enhancement of shell and tube heat exchanger using SnO_2-water and Ag-water nanofluids. *Therm. Sci. Eng. Appl.* **2020**, *12*, 041016. [CrossRef]

12. Li, J.; Yang, Z.; Hu, S.; Yang, F.; Duan, Y. Effects of shell-and-tube heat exchanger arranged forms on the thermo-economic performance of organic Rankine cycle systems using hydrocarbons. *Energy Convers. Manag.* **2020**, *203*, 112248. [CrossRef]
13. Miansari, M.; Jafarzadeh, A.; Toghraie, D. Thermal performance of a helical shell and tube heat exchanger without fin, with circular fins, and with V-shaped circular fins applying on the coil. *J. Therm. Anal. Calorim.* **2021**, *43*, 4273–4285. [CrossRef]
14. Bejan, A. Street network theory of organization in nature. *J. Adv. Transp.* **1996**, *30*, 85–107. [CrossRef]
15. Bejan, A. Constructal-theory network of conducting paths for cooling a heat generating volume. *Int. J. Heat Mass Transf.* **1997**, *40*, 799–816. [CrossRef]
16. Bejan, A. *Shape and Structure, from Engineering to Nature*; Cambridge University Press: Cambridge, UK, 2000.
17. Kim, S.; Lorente, S.; Bejan, A. *Design with Constructal Theory: Vascularized Composites for Volumetric Cooling*; ASME International: New York, NY, USA, 2008.
18. Lorenzini, G.; Moretti, S.; Conti, A. *Fin Shape Thermal Optimization Using Bejan's Constructal Theory*; Morgan & Claypool Publishers: San Francisco, CA, USA, 2011.
19. Chen, L.G. Progress in study on constructal theory and its applications. *Sci. China Tech. Sci.* **2012**, *42*, 505–524. [CrossRef]
20. Chen, L.G.; Feng, H.J. *Multi-Objective Constructal Optimization for Flow and Heat and Mass Transfer Processes*; Science Press: Beijing, China, 2017.
21. Bejan, A. Constructal law, twenty years after. *Proc. Rom. Acad. Ser. A Math. Phys. Tech. Sci. Inform. Sci.* **2018**, *18*, 309–311.
22. Chen, L.G.; Feng, H.J.; Xie, Z.H.; Sun, F.R. Progress of constructal theory in China over the past decade. *Int. J. Heat Mass Transf.* **2019**, *130*, 393–419. [CrossRef]
23. Lorente, S.; Bejan, A. Current trends in constructal law and evolutionary design. *Heat Transf.-Asian Res.* **2019**, *48*, 357–389. [CrossRef]
24. Bejan, A. *Freedom and Evolution: Hierarchy in Nature*; Springer Science and Business Media LLC: Berlin, Germany, 2020.
25. Chen, L.G.; Yang, A.B.; Feng, H.J.; Ge, Y.L.; Xia, S.J. Constructal designs for eight types of heat sinks. *Sci. China Technol. Sci.* **2020**, *63*, 1–33. [CrossRef]
26. Wu, Z.X.; Feng, H.J.; Chen, L.G.; Ge, Y.L. Performance optimization of a condenser in ocean thermal energy conversion (OTEC) system based on constructal theory and multi-objective genetic algorithm. *Entropy* **2020**, *22*, 641. [CrossRef]
27. Chen, L.G.; Wu, W.J.; Feng, H.J. *Constructal Design for Heat Conduction*; Book Publisher International: London, UK, 2021.
28. Bejan, A.; Almahmoud, H.; Gucluer, S. Evolutionary design of composite structures for thermal conductance and strength. *Int. Comm. Heat Mass Transf.* **2021**, *125*, 105293. [CrossRef]
29. Kuddusi, L.; Denton, J.C. Analytical solution for heat conduction problem in composite slab and its implementation in constructal solution for cooling of electronics. *Energy Convers. Manag.* **2007**, *48*, 1089–1105. [CrossRef]
30. Marck, G.; Harion, J.L.; Nemer, M.; Russeil, S.; Bougeard, D. A new perspective of constructal networks cooling a finite-size volume generating heat. *Energy Convers. Manag.* **2011**, *52*, 1033–1046. [CrossRef]
31. Tescari, S.; Mazet, N.; Neveu, P. Constructal theory through thermodynamics of irreversible processes framework. *Energy Convers. Manag.* **2011**, *52*, 3176–3188. [CrossRef]
32. Zhang, F.Y.; Feng, H.J.; Chen, L.G.; You, J.; Xie, Z.J. Constructal design of an arrow-shaped high thermal conductivity channel in a square heat generation body. *Entropy* **2020**, *22*, 475. [CrossRef] [PubMed]
33. Li, Y.L.; Feng, M.L. Optimal design of conductive natural branched pathways for cooling a heat-generating volume. *Heat Transf.* **2021**, *50*, 2571–2591. [CrossRef]
34. Hajmohammadi, M.R.; Poozesh, S.; Campo, A.; Nourazar, S.S. Valuable reconsideration in the constructal design of cavities. *Energy Convers. Manag.* **2013**, *66*, 33–40. [CrossRef]
35. Gonzales, G.V.; Lorenzini, G.; Isoldi, L.A.; Rocha, L.A.O.; dos Santos, E.D.; Silva Neto, A.J. Constructal design and simulated annealing applied to the geometric optimization of an isothermal double T-shaped cavity. *Int. J. Heat Mass Transf.* **2021**, *174*, 121268. [CrossRef]
36. Lu, Z.H.; Zhang, K.; Liu, J.X.; Li, F. Effect of branching level on the performance of constructal theory based Y-shaped liquid cooling heat sink. *Appl. Therm. Eng.* **2020**, *168*, 114824. [CrossRef]
37. Hazarika, S.A.; Deshmukhya, T.; Bhanja, D.; Nath, S. A novel optimum constructal fork-shaped fin array design for simultaneous heat and mass transfer application in a space-constrained situation. *Int. J. Therm. Sci.* **2020**, *150*, 106225. [CrossRef]
38. Wei, S.H.; Feng, H.J.; Chen, L.G.; Ge, Y.L. Constructal equivalent thermal resistance minimization for Tau-shaped fin. *Entropy* **2020**, *22*, 1206. [CrossRef] [PubMed]
39. Chen, C.; You, J.; Feng, H.J.; Chen, L.G. A multi-objective study on the constructal design of non-uniform heat generating disc cooled by radial- and dendritic-pattern cooling channels. *Sci. China Technol. Sci.* **2021**, *64*, 729–744. [CrossRef]
40. Hajmohammadi, M.R.; Salimpour, M.R.; Saber, M.; Campo, A. Detailed analysis for the cooling performance enhancement of a heat source under a thick plate. *Energy Convers. Manag.* **2013**, *76*, 691–700. [CrossRef]
41. Birinci, S.; Saglam, M.; Sarper, B.; Aydin, O. Constructal design of heat sources with different heat generation rates for the hot spot mitigation. *Int. J. Heat Mass Transf.* **2020**, *163*, 120472. [CrossRef]
42. Neveu, P.; Tescari, S.; Aussel, D.; Mazet, N. Combined constructal and exergy optimization of thermochemical reactors for high temperature heat storage. *Energy Convers. Manag.* **2013**, *71*, 186–198. [CrossRef]
43. Joshi, V.; Rathod, M.K. Constructal enhancement of thermal transport in latent heat storage systems assisted with fins. *Int. J. Therm. Sci.* **2019**, *145*, 105984. [CrossRef]

44. Wu, Z.X.; Feng, H.J.; Chen, L.G.; Tang, W.; Shi, J.Z.; Ge, Y.L. Constructal thermodynamic optimization for ocean thermal energy conversion system with dual-pressure organic Rankine cycle. *Energy Convers. Manag.* **2020**, *210*, 112727. [CrossRef]
45. Feng, H.J.; Wu, Z.X.; Chen, L.G.; Ge, Y.L. Constructal thermodynamic optimization for dual-pressure organic Rankine cycle in waste heat utilization system. *Energy Convers. Manag.* **2021**, *227*, 113585. [CrossRef]
46. Mosa, M.; Malley-Ernewein, A. Constructal design applications in buildings: Radiant cooling panels and thermochemical energy storage. *Heat Transf.* **2020**, *49*, 3981–3996. [CrossRef]
47. Rodrigues, G.C.; Lorenzini, G.; Victoria, L.C.; Vaz, I.S.; Rocha, L.A.O.; dos Santos, E.D.; Rodrigues, M.K.; da S D Estrada, E.; Isoldi, L.A. Constructal design applied to the geometric evaluation of a T-shaped earth-air heat exchanger. *Int. J. Sustain. Dev. Plan.* **2021**, *16*, 207–217. [CrossRef]
48. Pinto, V.T.; Cunha, M.L.; Martins, K.L.; Rocha, L.A.O.; de Vasconcellos Real, M.; dos Santos, E.D.; Isoldi, L.A. Geometric evaluation of steel plates subjected to uniform transverse load with rectangular or trapezoidal stiffeners by means constructal design method. *Int. J. Hydromechatron.* **2020**, *3*, 190–198. [CrossRef]
49. da Silveira, T.; Pinto, V.T.; Neufeld, J.P.S.; Pavlovic, A. Applicability evidence of constructal design in structural engineering: Case study of biaxial elasto-plastic buckling of square steel plates with elliptical cutout. *J. Appl. Comput. Mech.* **2021**, *7*, 922–934.
50. Cetkin, E. The effect of cooling on mechanical and thermal stresses in vascular structures. *J. Therm. Eng.* **2018**, *4*, 1855–1866. [CrossRef]
51. Dadsetani, R.; Sheikhzade, G.A.; Goodarzi, M.; Zeeshan, A. Thermal and mechanical design of tangential hybrid microchannel and high-conductivity inserts for cooling of disk-shaped electronic components. *J. Therm. Anal. Calorim.* **2021**, *143*, 2125–2133. [CrossRef]
52. Vargas, J.V.C.; Bejan, A. Thermodynamic optimization of finned crossflow heat exchangers for aircraft environmental control systems. *Int. J. Heat Fluid Flow* **2001**, *22*, 657–665. [CrossRef]
53. Bejan, A. Dendritic constructal heat exchanger with small-scale crossflows and larger-scales counterflows. *Int. J. Heat Mass Transf.* **2002**, *45*, 4607–4620. [CrossRef]
54. Silva, D.A.K.; Lorente, S.; Bejan, A. Constructal multi-scale tree-shaped heat exchanger. *J. Appl. Phys.* **2004**, *96*, 1709–1718. [CrossRef]
55. Silva, D.A.K.; Bejan, A. Dendritic counterflow heat exchanger experiments. *Int. J. Therm. Sci.* **2006**, *45*, 860–869. [CrossRef]
56. Zimparov, V.D.; Silva, D.A.K.; Bejan, A. Constructal tree-shaped parallel flow heat exchangers. *Int. J. Heat Mass Transf.* **2006**, *49*, 4558–4566. [CrossRef]
57. Azad, A.V.; Amidpour, M. Economic optimization of shell-and-tube heat exchanger based on constructal theory. *Energy* **2011**, *36*, 1087–1096. [CrossRef]
58. Yang, J.; Oh, S.R.; Liu, W. Optimization of shell-and-tube heat exchangers using a general design approach motivated by constructal theory. *Int. J. Heat Mass Transf.* **2014**, *77*, 1144–1154. [CrossRef]
59. Yang, J.; Fan, A.W.; Liu, W.; Jacobi, A.M. Optimization of shell-and-tube heat exchangers conforming to TEMA standards with designs motivated by constructal theory. *Energy Convers. Manag.* **2014**, *78*, 468–476. [CrossRef]
60. Mirzaei, M.; Hajabdollahi, H.; Fadakar, H. Multi-objective optimization of shell-and-tube heat exchanger by constructal theory. *Appl. Therm. Eng.* **2017**, *125*, 9–19. [CrossRef]
61. Manjunath, K.; Kaushik, S.C. Second law analysis of unbalanced constructal heat exchanger. *Int. J. Green Energy* **2014**, *11*, 173–192. [CrossRef]
62. Bejan, A.; Lorente, S.; Martins, L.; Meyer, J.P. The constructal size of a heat exchanger. *J. Appl. Phys.* **2017**, *122*, 064902. [CrossRef]
63. Hajabdollahi, H. Multi-objective optimization of plate fin heat exchanger using constructal theory. *Int. Commun. Heat Mass Transf.* **2019**, *108*, 104283. [CrossRef]
64. Ariyo, D.O.; Bello-Ochende, T. Constructal design of subcooled microchannel heat exchangers. *Int. J. Heat Mass Transf.* **2020**, *146*, 118835. [CrossRef]
65. Martins, L.S.; Ordonez, J.C.; Vargas, J.V.C.; Parise, J.A.R. Thermodynamic optimization of a regenerator heat exchanger. *Appl. Therm. Eng.* **2012**, *45*, 42–51. [CrossRef]
66. Bejan, A.; Lorente, S.; Kang, D.H. Constructal design of regenerators. *Int. J. Energy Res.* **2013**, *37*, 1509–1518. [CrossRef]
67. Bejan, A.; Lorente, S.; Anderson, R. Constructal underground designs for ground-coupled heat pumps. *Trans. ASME J. Sol. Energy Eng.* **2014**, *136*, 011019. [CrossRef]
68. Rodrigues, M.K.; Silva, D.B.R.; Vaz, J.; Rocha, L.A.O.; Santos, D.E.D.; Isoldi, L.A. Numerical investigation about the improvement of the thermal potential of an earth-air heat exchanger (EAHE) employing the constructal design method. *Renew. Energy* **2015**, *80*, 538–551. [CrossRef]
69. Cai, C.G.; Feng, H.J.; Chen, L.G.; Wu, Z.X.; Xie, Z.J. Constructal design of a shell-and-tube evaporator with ammonia-water working fluid. *Int. J. Heat Mass Transf.* **2019**, *135*, 541–547. [CrossRef]
70. Wu, Z.X.; Feng, H.J.; Chen, L.G.; Xie, Z.J.; Cai, C.G. Pumping power minimization of an evaporator in ocean thermal energy conversion system based on constructal theory. *Energy* **2019**, *181*, 974–984. [CrossRef]
71. Xie, Z.J.; Feng, H.J.; Chen, L.G.; Wu, Z.X. Constructal design for supercharged boiler evaporator. *Int. J. Heat Mass Transf.* **2019**, *138*, 571–579. [CrossRef]
72. Feng, H.J.; Xie, Z.J.; Chen, L.G.; Wu, Z.X.; Xia, S.J. Constructal design for supercharged boiler superheater. *Energy* **2020**, *191*, 116484. [CrossRef]

73. Tang, W.; Feng, H.J.; Chen, L.G.; Xie, Z.J.; Shi, J.Z. Constructal design for a boiler economizer. *Energy* **2021**, *223*, 120013. [CrossRef]
74. Gulotta, T.M.; Guarino, F.; Cellura, M.; Lorenzini, G. Constructal law optimization of a boiler. *Int. J. Heat Technol.* **2017**, *35*, 297–305. [CrossRef]
75. Gulotta, T.M.; Guarino, F.; Cellura, M.; Lorenzini, G. A constructal law optimization of a boiler inspired by life cycle thinking. *Therm. Sci. Eng. Prog.* **2018**, *6*, 380–387. [CrossRef]
76. Kim, Y.S.; Lorente, S.; Bejan, A. Constructal steam generator architecture. *Int. J. Heat Mass Transf.* **2009**, *52*, 2362–2369. [CrossRef]
77. Norouzi, E.; Amidpour, M. Optimal thermodynamic and economic volume of a heat recovery steam generator by constructal design. *Int. Commun. Heat Mass Transf.* **2012**, *39*, 1286–1292. [CrossRef]
78. Mehrgoo, M.; Amidpour, M. Constructal design and optimization of a dual pressure heat recovery steam generator. *Energy* **2017**, *124*, 87–99. [CrossRef]
79. Norouzi, E.; Amidpour, M.; Rezakazemi, M. Heat recovery steam generator: Constructal thermoeconomic optimization. *Appl. Therm. Eng.* **2019**, *148*, 747–753. [CrossRef]
80. Bejan, A.; Lee, J.; Lorente, S.; Kim, Y. The evolutionary design of condensers. *J. Appl. Phys.* **2015**, *117*, 125101. [CrossRef]
81. Li, B.T.; Xu, J.H.; Y, N.; Hong, J. Optimization design of grooved condenser wick structures in a vapor chamber for electronic cooling applications. *Struct. Multidiscipl. Optim.* **2019**, *61*, 1–19. [CrossRef]
82. Xu, W. Numerical and Experimental Studies of Vapor-Liquid Two-Phase Flow and Heat Transfer in Marine Condenser. Ph.D. Thesis, Harbin Engineering University, Harbin, China, 2015. (In Chinese)
83. Yang, S.M.; Tao, W.Q. *Heat Transfer*; Higher Education Press: Beijing, China, 2006. (In Chinese)
84. Li, Y.Q.; Liao, S.M.; Liu, G. Thermo-economic multi-objective optimization for a solar-dish Brayton system using NSGA-II and decision making. *Int. J. Electr. Power Energy Syst.* **2015**, *64*, 167–175. [CrossRef]
85. Ghorani, M.M.; Haghighi, M.H.S.; Riasi, A. Entropy generation minimization of a pump running in reverse mode based on surrogate models and NSGA-II. *Int. Commun. Heat Mass Transf.* **2020**, *118*, 104898. [CrossRef]
86. Ghazvini, M.; Pourkiaei, S.M.; Pourfayaz, F. Thermo-economic assessment and optimization of actual heat engine performance by implemention of NSGA II. *Renew. Energy Res. Appl.* **2020**, *1*, 235–245.
87. Wang, L.B.; Bu, X.B.; Li, H.S. Multi-objective optimization and off-design evaluation of organic rankine cycle (ORC) for low-grade waste heat recovery. *Energy* **2020**, *203*, 117809. [CrossRef]
88. Lee, U.; Park, S.; Lee, I. Robust design optimization (RDO) of thermoelectric generator system using non-dominated sorting genetic algorithm II (NSGA-II). *Energy* **2020**, *196*, 117090. [CrossRef]
89. Li, Y.Y.; Wang, S.Q.; Duan, X.B.; Liu, S.J.; Liu, J.P.; Hu, S. Multi-objective energy management for Atkinson cycle engine and series hybrid electric vehicle based on evolutionary NSGA-II algorithm using digital twins. *Energy Convers. Manag.* **2021**, *230*, 113788. [CrossRef]
90. Yusuf, A.; Bayhan, N.; Tiryaki, H.; Hamawandi, B.; Toprak, M.S.; Ballikaya, S. Multi-objective optimization of concentrated photovoltaic-thermoelectric hybrid system via non-dominated sorting genetic algorithm (NSGA II). *Energy Convers. Manag.* **2021**, *236*, 114065. [CrossRef]
91. Ahmadi, M.H.; Ahmadi, M.A.; Shafaei, A.; Ashouri, M.; Toghyani, S. Thermodynamic analysis and optimization of the Atkinson engine by using NSGA-II. *Int. J. Low-Carbon Technol.* **2016**, *11*, 317–324. [CrossRef]
92. Xu, Z.; Guo, Y.Q.; Mao, H.T.; Yang, F.Q. Configuration optimization and performance comparison of STHX-DDB and STHX-SB by a multi-objective genetic algorithm. *Energies* **2019**, *12*, 1794. [CrossRef]
93. Tang, C.Q.; Feng, H.J.; Chen, L.G.; Wang, W.H. Power density analysis and multi-objective optimization for a modified endoreversible simple closed Brayton cycle with one isothermal heat process. *Energy Rep.* **2020**, *6*, 1648–1657. [CrossRef]
94. Meng, J.H.; Wu, H.C.; Wang, T.H. Optimization of two-stage combined thermoelectric devices by a three-dimensional multi-physics model and multi-objective genetic algorithm. *Energies* **2019**, *12*, 2832. [CrossRef]
95. Abedinnezhad, S.; Ahmadi, M.H.; Pourkiaei, S.M.; Pourfayaz, F.; Mosavi, A.; Feidt, M.; Shamshirband, S. Thermodynamic assessment and multi-objective optimization of performance of irreversible Dual-Miller cycle. *Energies* **2019**, *12*, 4000. [CrossRef]
96. Sun, M.; Xia, S.J.; Chen, L.G.; Wang, C.; Tang, C.Q. Minimum entropy generation rate and maximum yield optimization of sulfuric acid decomposition process using NSGA-II. *Entropy* **2020**, *22*, 1065. [CrossRef]
97. Shi, S.S.; Ge, Y.L.; Chen, L.G.; Feng, F.J. Four objective optimization of irreversible Atkinson cycle based on NSGA-II. *Entropy* **2020**, *22*, 1150. [CrossRef]
98. Chen, L.G.; Tang, C.Q.; Feng, H.J.; Ge, Y.L. Power, efficiency, power density and ecological function optimizations for an irreversible modified closed variable-temperature reservoir regenerative Brayton cycle with one isothermal heating process. *Energies* **2020**, *13*, 5133. [CrossRef]
99. Zhang, L.; Chen, L.G.; Xia, S.J.; Ge, Y.L.; Wang, C.; Feng, H.J. Multi-objective optimization for helium-heated reverse water gas shift reactor by using NSGA-II. *Int. J. Heat Mass Transf.* **2020**, *148*, 119025. [CrossRef]
100. Jankowski, M.; Borsukiewicz, A.; Hooman, K. Development of decision-making tool and pareto set analysis for bi-objective optimization of an ORC power plant. *Energies* **2020**, *13*, 5280. [CrossRef]
101. Tang, C.Q.; Chen, L.G.; Feng, H.J.; Ge, Y.L. Four-objective optimizations for an improved irreversible closed modified simple Brayton cycle. *Entropy* **2021**, *23*, 282. [CrossRef] [PubMed]
102. Yang, J.Y.; Gao, L.; Ye, Z.H.; Hwang, Y.H.; Chen, J.P. Binary-objective optimization of latest low-GWP alternatives to R245fa for organic Rankine cycle application. *Energy* **2021**, *216*, 119336. [CrossRef]

103. Shi, S.S.; Chen, L.G.; Ge, Y.L.; Feng, F.J. Performance optimizations with single-, bi-, tri- and quadru-objective for irreversible Diesel cycle. *Entropy* **2021**, *23*, 826. [CrossRef] [PubMed]
104. Shi, S.S.; Chen, L.G.; Ge, Y.L.; Feng, F.J. Performance optimizations with single-, bi-, tri- and quadru-objective for irreversible Atkinson cycle with nonlinear variation of working fluid's specific heat. *Energies* **2021**, *14*, 4175. [CrossRef]
105. Zhang, Z.M.; Feng, H.J.; Chen, L.G.; Ge, Y.L. Multi-objective constructal design for compound heat dissipation channels in a three-dimensional trapezoidal heat generation body. *Int. Commun. Heat Mass Transf.* **2021**, *127*, 105584. [CrossRef]
106. Gong, Q.R.; Ge, Y.L.; Chen, L.G.; Shi, S.S.; Feng, H.J. Performance analyses and four-objective optimizations of an irreversible rectangular cycle. *Entropy* **2021**, *23*. in press.